

ADAPTIVE OBSERVER DESIGN FOR A LI-ION CELL BASED ON COUPLED ELECTROCHEMICAL-THERMAL MODEL

Satadru Dey
Clemson University
Greenville, SC-29607, USA
satadrd@clemson.edu

Beshah Ayalew
Clemson University
Greenville, SC-29607, USA
beshah@clemson.edu

Pierluigi Pisu
Clemson University
Greenville, SC-29607, USA
pisup@clemson.edu

ABSTRACT

Accurate real-time knowledge of battery internal states and physical parameters is of the utmost importance for intelligent battery management. Electrochemical models are arguably more accurate in capturing physical phenomena inside the cells compared to their data-driven or equivalent circuit based counterparts. Moreover, consideration of the coupling between electrochemical and thermal dynamics can be potentially beneficial for accurate estimation. In this paper, a nonlinear adaptive observer design is presented based on a coupled electrochemical-thermal model for a Li-ion cell. The proposed adaptive observer estimates distributed Li-ion concentrations, lumped temperature and some electrochemical parameters simultaneously. The observer design is split into two separate parts to simplify the design procedure and gain tuning. These separate parts are designed based on Lyapunov's stability analysis guaranteeing the convergence of the combined state-parameter estimates. Simulation studies are provided to demonstrate the effectiveness of the scheme.

NOMENCLATURE

A Current collector area (cm^2)
 A_s Cell surface area exposed to surroundings (cm^2)
 a_s^\pm Specific surface area (cm^2/cm^3)
 c_e Electrolyte phase Li-ion concentration (mol/cm^3)
 c_s^\pm Solid phase Li-ion concentration (mol/cm^3)
 $c_{s,e}^\pm$ Solid-phase Li-ion surface-concentration (mol/cm^3)
 $c_{s,max}^\pm$ Solid-phase Li-ion max. concentration (mol/cm^3)
 D_s^\pm Diffusion coefficient in solid phase (cm^2/s)

$D_{s,ref}^\pm$ Diffusion coefficient at T_{ref} (cm^2/s)
 E_K^\pm Activation Energy of diffusion coefficient (J/mol)
 E_{Ds}^\pm Activation Energy of reaction rate constant (J/mol)
 h Heat transfer coefficient of the cell ($\text{W}/\text{cm}^2\text{-K}$)
 F Faraday's constant (C/mol)
 I Current (A)
 K^\pm Reaction rate constant ($\text{cm}^{2.5}/\text{mol}^{0.5}/\text{s}$)
 K_{ref}^\pm Reaction rate constant at T_{ref} ($\text{cm}^{2.5}/\text{mol}^{0.5}/\text{s}$)
 L^\pm Length of the cell (cm)
 r Radial coordinate (cm)
 R Radius of solid active particle (cm)
 \bar{R} Universal Gas Constant (J/mol-K)
 R_f Contact film resistance (Ω)
 T Temperature (K)
 T_{ref} Reference temperature (K)
 T_∞ Temperature of cooling fluid (K)
 U^\pm Open circuit potential (V)
 α^\pm Charge transfer coefficient
 ρ Cell density (g/cm^3)
 v Cell volume (cm^3)
 C_p Specific heat capacity (J/g-K)
 Superscript
 \pm positive/negative electrode

INTRODUCTION

Li-ion batteries are becoming increasingly popular in electrified transportation and stationary renewable energy storage applications due to their beneficial features such as

higher power-to-weight ratio, low self-discharge and less environmental impact. However, safety and reliability are still key concerns for this technology. One aspect of overcoming these issues is proper design of Battery Management Systems (BMS), which require precise knowledge of battery internal information like State-of-Charge (SOC) and State-of-Health (SOH).

The main challenge for meeting these requirements is that, in general, the only available information in real-time is boundary measurement of voltage, current and temperature. This fact leads to the necessity of reliable estimation algorithms that determine the internal information in the Li-ion cells from these limited measurements and available models. Moreover, there are two specific challenges in SOC and SOH estimation of Li-ion cells. The first arises from the spatially distributed nature of Li-ion concentrations inside the electrodes. The second is parametric uncertainty as the parameters vary with Li-ion chemistry, cell-to-cell manufacturing variability and time (including shelf-time). In this paper, we address these challenges. Specifically, we propose an electrochemical-thermal model-based adaptive algorithm for online simultaneous SOC and parameter estimation. In addition to improving the accuracy of SOC estimation, online parameter estimates can be used as State-of-Health (SOH) indicators.

The different adaptive estimation algorithms proposed for Li-ion batteries can be broadly classified based on type of model used: 1) Data-driven model [2],[3], 2) Equivalent circuit model (ECM) [4],[5],[6], and 3) Electrochemical model. Although data-driven and ECM based approaches are simple in implementation and design, the downsides are extensive parameterization and lack of physical meaning of the parameters.

Electrochemical model-based approaches, built on porous electrode and concentrated solution theories, are more accurate compared to conventional data-driven or ECM models [7]. However, full-order electrochemical model (also known as pseudo-two-dimensional (P2D) model) consists of nonlinear coupled Partial Differential Equations (PDE) [8]. The complex structure of the P2D model has spurred different model reductions in the literature for subsequent use in estimator design. For example, a residue grouping with a Kalman filter was used in [9] and a constant electrolyte concentration assumption with output injection observer was used in [10]. A single Particle Model (SPM) with the electrodes approximated as spherical particles was used for SOC estimator design in [11], [12], [13]. The present authors proposed SPM based two nonlinear observer designs for the SOC estimation in [14].

Although the SOC estimation problem is well investigated for electrochemical models, adaptive estimation or the problem of simultaneous state and parameter estimation is relatively less explored. Some of the existing works use multi-rate particle filtering (PF) approach [15], unscented Kalman filter (UKF) approach [16], iterated extended Kalman filter (IEKF) approach [17],[18]. However, it is difficult to theoretically verify the stability properties of the estimators designed by UKF/PF/IEKF. In [19], an adaptive PDE observer framework is

presented. However, combined stability properties of the state and parameter estimators are not verified analytically. The authors of the present paper proposed a sliding mode observer based adaptive approach in [20] for estimation of SOC and physical parameters (namely, diffusion coefficient and film resistance). However, the approach requires the initial value of film resistance to be known with certain accuracy.

Almost all of the adaptive estimation approaches cited above consider only electrochemical dynamics of the cell ignoring the thermal dynamics. However, in reality there is a bi-directional coupling between the electrochemical and thermal dynamics of a Li-ion cell. In [10] and [21], numerical and experimental results of SOC observer with coupled electrochemical-thermal dynamics, has shown that inclusion of the thermal model in the observer has a significant potential to improve the estimation accuracy. This also makes sense from physical point of view due to the bi-directional coupling described as follows: in electrochemical model the open circuit potential and some parameters are affected by temperature changes whereas in the thermal model, the electrochemical overpotential and open circuit potential contribute to heat generation [25].

To summarize, most of the current adaptive estimation schemes have the following issues 1) thermal coupling is not considered along with electrochemical model, 2) there is a lack of theoretical verification of convergence for the combined state-parameter estimation schemes.

In this paper we address these issues by proposing a Lyapunov-based nonlinear adaptive observer design based on a combined electrochemical-thermal model of a Li-ion cell. We also provide an analytical proof of convergence for the overall adaptive scheme combining state and parameter estimators. We utilize single particle electrochemical model (SPM) along with lumped thermal dynamics [22]. The parametric uncertainty in the model is assumed to be arisen from unknown diffusion coefficient, film resistance [23] and active material volume fraction. These three parameters will be estimated along with the SOC using adaptive laws and can subsequently be used as SOH indicators. As will be detailed below, the proposed approach is simple in design and implementation and is computationally efficient.

The rest of the paper is organized as follows. In the next section, the adopted electrochemical and thermal modeling of Li-ion cell is discussed. Then, detailed description of the adaptive scheme is provided along with systematic approaches for the selection of observer gains. Next, results and discussions are provided based on simulation studies. Finally, the concluding remarks are summarized.

LI-ION CELL ELECTROCHEMICAL-THERMAL MODEL

A reduced order electrochemical model of Li-ion cell known as Single Particle Model (SPM) [11], [12] is adopted here for observer design. Essentially, SPM consists of two linear diffusion PDEs for Li-ion mass conservation in both electrodes given by (1) and nonlinear voltage map derived from

Butler-Volmer kinetics given by (2), assuming volume-averaged current along the electrodes.

$$\frac{\partial c_s^\pm}{\partial t} = \frac{D_s^\pm(T)}{r^2} \frac{\partial}{\partial r} \left(r^2 \frac{\partial c_s^\pm}{\partial r} \right)$$

$$\left. \frac{\partial c_s^\pm}{\partial r} \right|_{r=0} = 0, \quad \left. \frac{\partial c_s^\pm}{\partial r} \right|_{r=R} = \frac{\pm I}{a_s^\pm F D_s^\pm(T) A L^\pm} \quad (1)$$

$$V = \frac{\bar{R}T}{\alpha^+ F} \sinh^{-1} \left(\frac{I}{2a_s^+ AL^+ K^+(T) \sqrt{c_e c_{s,e}^+ (c_{s,max}^+ - c_{s,e}^+)}} \right) - \frac{\bar{R}T}{\alpha^- F} \sinh^{-1} \left(\frac{I}{2a_s^- AL^- K^-(T) \sqrt{c_e c_{s,e}^- (c_{s,max}^- - c_{s,e}^-)}} \right) + U^+(c_{s,e}^+, T) - U^-(c_{s,e}^-, T) - R_f I \quad (2)$$

where U^+ and U^- are the open circuit potentials as functions of Li-ion surface concentration and temperature, c_s^\pm is the Li-ion concentration of the positive and negative electrode, V is the output voltage and I is the input current. The reader may refer to nomenclature above for the definitions of the rest of the variables.

Along with the electrochemical SPM model, the following lumped thermal model derived from the energy balance of the cell, is considered [22] and is given by:

$$\rho v C_p \frac{dT}{dt} = I \left(U^+(c_{s,e}^+, T) - U^-(c_{s,e}^-, T) - V - T \left(\frac{\partial U^+}{\partial T} - \frac{\partial U^-}{\partial T} \right) \right) - h A_s (T - T_\infty) \quad (3)$$

where T is the temperature and $\frac{\partial U^+}{\partial T}$ and $\frac{\partial U^-}{\partial T}$ are the changes in open circuit potentials due to temperature change. Note that, $\frac{\partial U^\pm}{\partial T}$ are functions of c_s^\pm only [22]. The previously mentioned coupling between the electrochemical and thermal model can be seen in (1), (2) and (3). The temperature affects the open circuit potential and overpotential terms in the voltage expression (2) whereas changes in the open circuit potential contribute to the heat generation in (3). Moreover, some electrochemical parameters have Arrhenius' correlation type dependence on temperature. In this study, we assume that the solid phase diffusion coefficients (D_s^\pm) and the reaction rate constants (K^\pm) show such dependence [22], as given by:

$$K^\pm(T) = K_{ref}^\pm \exp \left(\frac{E_K^\pm}{\bar{R}} \left(\frac{1}{T} - \frac{1}{T_{ref}} \right) \right)$$

$$D_s^\pm(T) = D_{s,ref}^\pm \exp \left(\frac{E_{Ds}^\pm}{\bar{R}} \left(\frac{1}{T} - \frac{1}{T_{ref}} \right) \right) \quad (4)$$

where T_{ref} is reference temperature, K_{ref}^\pm and $D_{s,ref}^\pm$ are the parameter values at that reference temperature. In this study we use the following approximation of the open circuit potential expression [22]:

$$U^\pm(c_{s,e}^\pm, T) \approx U^\pm(c_{s,e}^\pm, T_{ref}) + \frac{\partial U^\pm}{\partial T} (T - T_{ref}) \quad (5)$$

MODEL REDUCTION & FINITE-DIMENSIONAL APPROXIMATION

One of the challenges in Li-ion cell estimation is weak observability of SPM states via differential voltage measurement [12]. Different approaches have been proposed in literature to resolve this issue. In [12], Li-ion concentration in the negative electrode is computed using an algebraic function of positive electrode concentration based on stoichiometry points of the electrodes. In [13], the positive electrode concentration is approximated as an algebraic function of the negative electrode concentration based on conservation of Li-ions. In this paper, we follow the approach in [13] for model reduction to get an observable single PDE describing negative electrode diffusion dynamics along with a nonlinear output voltage map.

Next, we attempt to get a finite dimensional approximation of the reduced PDE using method of lines technique by approximating the spatial derivatives with finite central difference method. An illustration of SPM with discretization is shown in Fig. 1.

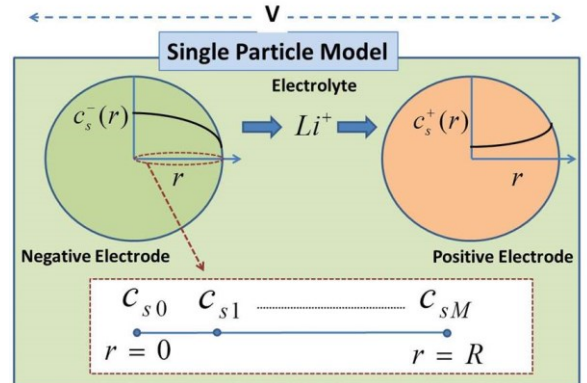


Figure 1: Illustration of SPM with Discretized Nodes

The resulting ODEs are given as follows:

$$\dot{c}_{s0} = -3ac_{s0} + 3ac_{s1}$$

$$\dot{c}_{sm} = \left(1 - \frac{1}{m}\right) ac_{s(m-1)} - 2ac_{sm} + \left(1 + \frac{1}{m}\right) ac_{s(m+1)}$$

$$\dot{c}_{sM} = \left(1 - \frac{1}{M}\right) ac_{s(M-1)} - \left(1 - \frac{1}{M}\right) ac_{sM} - \left(1 + \frac{1}{M}\right) bl \quad (6)$$

with $m = 1, \dots, (M - 1)$, discretization step $\Delta = R/M$, $a = D_s^- / \Delta^2$, $b = 1/a_s^- F \Delta A L^-$. Bulk SOC of the cell, which is related to the energy capacity, can be computed by volume averaging the node concentrations (c_{si}). The surface concentration c_{sM} describes the surface SOC, which is related to instantaneous power capacity. The voltage equation can be derived from (2) by substituting $c_{s,e}^- = c_{sM}$ and $c_{s,e}^+ = k_1 c_{sM} + k_2$ where k_1 and k_2 are constants in the algebraic relationship between positive and negative electrode Li-ion concentrations. These constants can be derived considering the conservation of Li-ions [13].

The cell thermal dynamics given by (3) is already in lumped ODE form and will be used as it is.

ESTIMATION PROBLEM

State-space Model Formulation & Analysis

The finite-dimensional state-space model for the Li-ion cell can be assembled from (6) and (3) along with the output voltage map is formed using (2). A compact form of the state-space model is:

$$\begin{aligned} \dot{x}_1 &= \theta f_1(x_2) A x_1 + B u \\ \dot{x}_2 &= u f_2(x_{1M}, x_2, y_1) - k(x_2 - x_{2\infty}) \\ y_1 &= h(x_{1M}, x_2, u) - R_f u \\ y_2 &= x_2 \end{aligned} \quad (7)$$

where $x_1 = [c_{s1}, \dots, c_{sM}]^T \in R^M$ is the state vector describing Li-ion concentrations at various nodes, $x_{1M} = x_1(M) = c_{sM} \in R$ is the surface concentration state, $x_2 \in R$ is temperature state and $x_{2\infty} \in R$ is the coolant/ambient temperature, $\theta = D_{s,ref}^- / \Delta^2 \in R$ is the scalar parameter related to the diffusion coefficient, $R_f \in R$ is the film resistance, $y_1 \in R$ is the measured voltage, $y_2 \in R$ is the measured temperature, $u \in R$ is the input current, $f_1: R \rightarrow R$ is a scalar function of the temperature given by the exponential term in Arrhenius equation (4), $A \in R^{M \times M}$ is the tri-diagonal matrix formed from (6), $B = [0, \dots, 0, B_M]^T \in R^{M \times 1}$ is a column vector formed by (6) where $B_M = 1/a_s^- F \Delta A L^-$, $f_2: R^3 \rightarrow R$ is a scalar function formed by (3), $k \in R$ is a scalar parameter, $h: R^3 \rightarrow R$ is a scalar function derived from voltage map. Note that, the zero-th node c_{s0} dynamics is neglected in (7) as keeping that dynamics leads to the unobservability. However, removing c_{s0} dynamics from the model does not lead to any information loss as it can be easily reconstructed from c_{s1} information.

We make the following observations of the system described in (7) which will be exploited later for design:

Observation I: The A matrix in (7) is a negative semi-definite matrix with eigen-values $\lambda(A) = [0, -\lambda_1, \dots, -\lambda_{M-1}]^T$ where $\lambda_i > 0$.

Observation II: The functions f_1 , f_2 and h are bounded within the operating range of the cell which means the function

outputs are finite given the function arguments are finite. Moreover, the function f_1 is always positive.

Observation III: The states of (7) are locally observable from the outputs as can be verified from local linearization of (7) at different points of the operating regime.

Observation IV: The output function y_1 is a strictly increasing function of the surface concentration state x_{1M} given any input current and temperature. The trend of output voltage (y_1) as a function of x_{1M} is given in Fig. 2 for a given current and temperature. Based on this observation, the following fact can be inferred: In the x_{1M} space, given any constant $u = u^*$ and $x_2 = x_2^*$, for two different values $x_{1M}^{(1)}$ and $x_{1M}^{(2)}$, we have $y_1^{(1)} = h^{(1)}(x_{1M}^{(1)}, x_2^*, u^*) - R_f u^*$ and $y_1^{(2)} = h^{(2)}(x_{1M}^{(2)}, x_2^*, u^*) - R_f u^*$. Now, using the strictly increasing property, we can write that:

$$\begin{aligned} \text{sgn}(y_1^{(1)} - y_1^{(2)}) &= \text{sgn}(x_{1M}^{(1)} - x_{1M}^{(2)}) \\ \Rightarrow \text{sgn}(h^{(1)}(x_{1M}^{(1)}, x_2^*, u^*) - h^{(2)}(x_{1M}^{(2)}, x_2^*, u^*)) \\ &= \text{sgn}(x_{1M}^{(1)} - x_{1M}^{(2)}) \end{aligned}$$

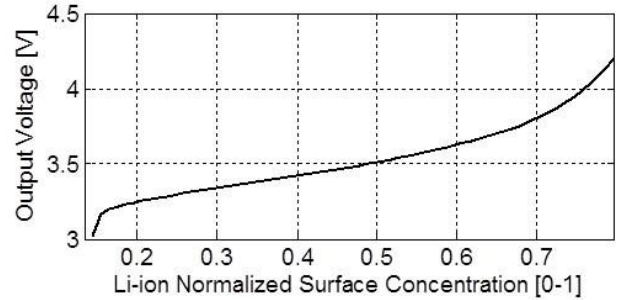


Figure 2: Output Voltage (y_1) as a Function of Surface Concentration (x_{1M})

Estimation Problem Formulation

State Estimation: The state estimation problem consists of estimating elements of x_1 , which are the Li-ion concentrations at various nodes and temperature state x_2 . Note that, x_{1M} indicates surface SOC. Bulk SOC can be computed from the full state vector x_1 information using the volume averaging formula:

$$SOC_{Bulk} = \frac{1}{4\pi R^3 c_{s,max}^-} \int_0^R 4\pi r^2 c_s^-(r, t) dr \quad (8)$$

Parameter Estimation: In this work, we assume the model uncertainty arises from the following parameters.

Diffusion coefficient: This leads to uncertain θ in (7).

Film resistance: This leads to uncertain R_f in (7).

Active material volume fraction of negative electrode: This leads to uncertainty in active surface area (a_s^-) as $a_s^- = 3\varepsilon_s/R$ where ε_s is the active material volume fraction. Note that, a_s^- is present both in matrix B and function h in (7). However, we observed via sensitivity analysis that error in a_s^- parameter has

negligible effect on function h whereas it significantly impacts the B matrix. Therefore, uncertainty due to a_s^- is assumed to be translated into uncertainty in B matrix only or specifically in B_M which is the only non-zero element in B . This is similar to the uncertainty in the boundary input coefficient assumed in [19].

These three parameters need to be estimated along with the states. Note that, besides improving the accuracy of the state estimates, the information on these parameters can also be used as an indicator for the SOH of the cell [23], [24].

ADAPTIVE OBSERVER DESIGN

The design goal of the adaptive observer is to estimate the states (x_1, x_2) and uncertain parameters (θ, R_f, B_M) using available measurements (y_1, y_2, u) . Except for the three uncertain parameters mentioned above, all the other model parameters and functions are assumed to be known.

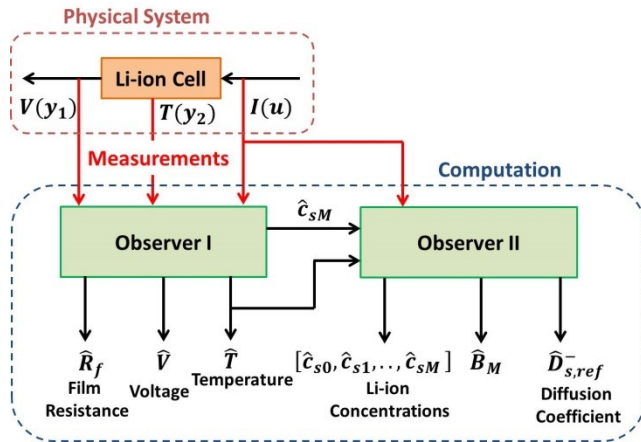


Figure 3: Adaptive Observer Scheme

A schematic of the overall adaptive observer scheme is shown in Fig. 3. In this work, we split the overall observer design into two parts. The Observer I computes estimates of the surface concentration (\hat{x}_{1M}), temperature (\hat{x}_2) and film resistance parameter (\hat{R}_f) utilizing the measurements of voltage (y_1) and temperature (y_2). The Observer II uses the estimates of surface concentration (\hat{x}_{1M}) and temperature (\hat{x}_2) from the Observer I and subsequently estimates the full concentration state vector (x_1), diffusion coefficient (θ) and B matrix parameter (B_M). Note that, in Observer II, the measured temperature value can be used instead of the estimated temperature. However, in this case we are using the estimated temperature which is a filtered version of the noisy measured temperature.

The motivation behind splitting the design into two parts instead of designing the full order observer at once lies in the simplification of the design procedure. Essentially, the full state and parameter vector is separated into two parts. The first part consists of the surface concentration and temperature states which are directly related to the available measurements (y_1, y_2) and film resistance parameter which is multiplied by

the measured current; the second part consists of the rest of the states and parameters. Then the design is done in a cascaded manner where the Observer I estimates the first part and feeds it to the Observer II which subsequently estimates the second part. Apart from simplification of design, this cascaded approach also makes tuning of the observer gains easier.

Design of Observer I

In this part of the design, we use a reduced-order system considering the partial dynamics given in (7). The partial dynamics can be written as:

$$\begin{aligned} \dot{R}_f &= 0 \\ \dot{x}_{1M} &= \theta f_1(x_2)A_1x_{1(M-1)} + \theta f_1(x_2)A_2x_{1M} + B_M u \\ \dot{x}_2 &= u f_2(x_{1M}, x_2, y_1) - k(x_2 - x_{2\infty}) \\ y_1 &= h(x_{1M}, x_2, u) - R_f u \\ y_2 &= x_2 \end{aligned} \quad (9)$$

where $x_{1(M-1)} \in R^{M-1}$ is the rest of the state vector x_1 except x_{1M} , R_f is the unknown parameter augmented in the state vector, A_1 and A_2 are the partitioned matrices originating from extracting the last row of the x_1 dynamics in (7). Note that, the reduced order system (9) is an uncertain system due to uncertainties in $x_{1(M-1)}$, θ and B_M .

The form of the observer is chosen as:

$$\begin{aligned} \dot{\hat{x}}_{1M} &= \hat{\theta} f_1(\hat{x}_2)A_1\hat{x}_{1(M-1)} + \hat{\theta} f_1(\hat{x}_2)A_2\hat{x}_{1M} + \hat{B}_M u \\ &\quad + L_1(y_1 - \hat{y}_1) \\ \dot{\hat{x}}_2 &= u f_2(\hat{x}_{1M}, \hat{x}_2, y_1) - k(\hat{x}_2 - x_{2\infty}) + L_2(y_2 - \hat{y}_2) \\ \hat{y}_1 &= h(\hat{x}_{1M}, \hat{x}_2, u) - \hat{R}_f u \\ \hat{y}_2 &= \hat{x}_2 \end{aligned} \quad (10)$$

The error dynamics can be written as:

$$\begin{aligned} \dot{\tilde{x}}_{1M} &= F_1 - L_1\tilde{y}_1 \\ \dot{\tilde{x}}_2 &= u f_2 - k\tilde{x}_2 - L_2\tilde{y}_2 \\ \dot{\tilde{y}}_1 &= \tilde{h} - \tilde{R}_f u \\ \dot{\tilde{y}}_2 &= \tilde{x}_2 \end{aligned} \quad (11)$$

where

$$\begin{aligned} F_1 &= \theta f_1(x_2)A_1x_{1(M-1)} + \theta f_1(x_2)A_2x_{1M} - \hat{\theta} f_1(\hat{x}_2)A_1\hat{x}_{1(M-1)} \\ &\quad - \hat{\theta} f_1(\hat{x}_2)A_2\hat{x}_{1M} + \hat{B}_M u \\ \tilde{h} &= h(x_{1M}, x_2, u) - h(\hat{x}_{1M}, \hat{x}_2, u) \\ f_2 &= f_2(x_{1M}, x_2, y_1) - f_2(\hat{x}_{1M}, \hat{x}_2, y_1) \\ \tilde{R}_f &= R_f - \hat{R}_f, \tilde{B}_M = B_M - \hat{B}_M, \tilde{x}_1 = x_1 - \hat{x}_1, \tilde{x}_2 = x_2 - \hat{x}_2 \\ \tilde{y}_1 &= y_1 - \hat{y}_1, \tilde{y}_2 = y_2 - \hat{y}_2 \\ \text{and } L_1, L_2 &\text{ are observer gains to be determined.} \end{aligned}$$

To analyze the stability of the error dynamics, the following Lyapunov function candidate has been chosen.

$$V = \frac{1}{2} \tilde{x}_{1M}^2 + \frac{1}{2} \tilde{x}_2^2 + \frac{1}{2} \tilde{R}_f^2$$

Taking the derivative of the Lyapunov function candidate,

$$\begin{aligned}\dot{V} &= \tilde{x}_{1M}\dot{\tilde{x}}_{1M} + \tilde{x}_2\dot{\tilde{x}}_2 + \tilde{R}_f\dot{\tilde{R}}_f \\ \Rightarrow \dot{V} &= \tilde{x}_{1M}(F_1 - L_1\tilde{y}_1) + \tilde{x}_2(uf_2^f - k\tilde{x}_2 - L_2\tilde{y}_2) - \tilde{R}_f\dot{\tilde{R}}_f \\ \Rightarrow \dot{V} &= \tilde{x}_{1M}(F_1 - L_1(\tilde{h} - \tilde{R}_f u)) + \tilde{x}_2(uf_2^f - k\tilde{x}_2 - L_2\tilde{y}_2) \\ &\quad - \tilde{R}_f\dot{\tilde{R}}_f \\ \Rightarrow \dot{V} &= \tilde{x}_{1M}(F_1 - L_1\tilde{h}) + L_1\tilde{x}_{1M}\tilde{R}_f u \\ &\quad + \tilde{x}_2(uf_2^f - k\tilde{x}_2 - L_2\tilde{y}_2) - \tilde{R}_f\dot{\tilde{R}}_f\end{aligned}$$

According to Observation IV we have $\text{sgn}(\tilde{h}) = \text{sgn}(\tilde{x}_{1M})$ which implies that $\tilde{x}_{1M}\tilde{h} > 0$ or equivalently, $\tilde{x}_{1M}\tilde{h} = |\tilde{x}_{1M}||\tilde{h}|$.

Note: Here $\tilde{h} = h(x_{1M}, x_2, u) - h(\hat{x}_{1M}, \hat{x}_2, u)$ is not only a function of \tilde{x}_{1M} but also a function of \tilde{x}_2 . However, it is observed that effect of temperature on h is much less than that of the surface concentration x_{1M} . Moreover, in reality the temperature measurement is always available which means \tilde{x}_2 will always be of smaller magnitude, therefore having negligible effect on \tilde{h} . Therefore, we can safely apply Observation IV in this case even with temperature estimation error $\tilde{x}_2 \neq 0$ identically.

Using the above observation and $\tilde{y}_2 = \tilde{x}_2$, \dot{V} can be written as:

$$\begin{aligned}\dot{V} &= (\tilde{x}_{1M}F_1 - L_1|\tilde{x}_{1M}||\tilde{h}|) + (uf_2^f\tilde{x}_2 - (k + L_2)\tilde{x}_2^2) \\ &\quad + L_1\tilde{x}_{1M}\tilde{R}_f u - \tilde{R}_f\dot{\tilde{R}}_f\end{aligned}$$

Using the inequality, $ab \leq |ab| = |a||b|$,

$$\begin{aligned}\dot{V} &\leq (|\tilde{x}_{1M}||F_1| - L_1|\tilde{x}_{1M}||\tilde{h}|) \\ &\quad + (|uf_2^f||\tilde{x}_2| - (k + L_2)|\tilde{x}_2|^2) + L_1\tilde{x}_{1M}\tilde{R}_f u - \tilde{R}_f\dot{\tilde{R}}_f \\ \Rightarrow \dot{V} &\leq |\tilde{x}_{1M}|(|F_1| - L_1|\tilde{h}|) \\ &\quad + |\tilde{x}_2|(|uf_2^f| - (k + L_2)|\tilde{x}_2|) + L_1\tilde{x}_{1M}\tilde{R}_f u - \tilde{R}_f\dot{\tilde{R}}_f\end{aligned}$$

Now we can choose the following adaptive law for the estimation of film resistance:

$$\dot{\tilde{R}}_f = -L_3 \text{sgn}(u) \text{sgn}(\tilde{y}_1) \Rightarrow \dot{\tilde{R}}_f = -L_3 \text{sgn}(u) \text{sgn}(\tilde{h} - \tilde{R}_f u)$$

Therefore, the \dot{V} equation becomes:

$$\begin{aligned}\dot{V} &\leq |\tilde{x}_{1M}|(|F_1| - L_1|\tilde{h}|) \\ &\quad + |\tilde{x}_2|(|uf_2^f| - (k + L_2)|\tilde{x}_2|) \\ &\quad + L_1\tilde{x}_{1M}\tilde{R}_f u + L_3\tilde{R}_f \text{sgn}(u) \text{sgn}(\tilde{h} - \tilde{R}_f u)\end{aligned}\quad (12)$$

Considering the first term in right hand side of (12), if we choose sufficiently high positive L_1 , $|\tilde{x}_{1M}|(|F_1| - L_1|\tilde{h}|)$ will be negative given the condition $L_1 > |F_1|/|\tilde{h}|$. This means that $|\tilde{x}_{1M}|$ will always decrease till this condition is true. However, \tilde{x}_{1M} will not go to zero as it will stay on some bounded manifold in that error space that is determined by the value of L_1 and the magnitude of $|F_1|$.

A similar argument can be made for the second term in right hand side of (12). Based on the selection of some high positive L_2 , $|\tilde{x}_2|$ will decrease till the condition $L_2 > |uf_2^f|/|\tilde{x}_2|$ is true. Subsequently, $|\tilde{x}_2|$ will stay on some bounded manifold determined by the value of L_2 and magnitude of $|uf_2^f|$.

Now consider the third term on the right hand side of (12). Under the condition $|\tilde{h}| < |\tilde{R}_f u|$, we can write $\text{sgn}(\tilde{h} - \tilde{R}_f u) = \text{sgn}(-\tilde{R}_f u) = -\text{sgn}(\tilde{R}_f) \text{sgn}(u)$. This makes the third term, $L_1\tilde{x}_{1M}\tilde{R}_f u + L_3\tilde{R}_f \text{sgn}(u) \text{sgn}(\tilde{h} - \tilde{R}_f u) = L_1\tilde{x}_{1M}\tilde{R}_f u - L_3\tilde{R}_f \text{sgn}(\tilde{R}_f)$. Using the inequality, $ab \leq |ab| = |a||b|$, the above expression becomes $|\tilde{R}_f|(L_1|\tilde{x}_{1M}||u| - L_3)$. Selection of some high positive L_3 will make $|\tilde{R}_f|$ to decrease till one of the two conditions $L_1|\tilde{x}_{1M}||u| < L_3$ or $|\tilde{h}| < |\tilde{R}_f u|$ is true. Similar to other error variables, $|\tilde{R}_f|$ will not go to zero but stay on some bounded manifold in that error space that is determined by the values of L_3, L_1 and magnitude of $|\tilde{x}_{1M}|$ and $|\tilde{h}|$. Note that, convergence of \tilde{R}_f depends on $u \neq 0$ condition. Therefore, to make \tilde{R}_f to go to a certain bounded value some persistence of input current excitation is required.

From this Lyapunov analysis, we can conclude that based on some selection of high observer gains, the errors $\tilde{x}_{1M}, \tilde{x}_2$ and \tilde{R}_f will go to some bounded manifold. However, it can be shown that for sufficiently high values of L_1 and L_2 , the steady-state value of \tilde{x}_{1M} and \tilde{x}_2 can be made negligibly small. These estimates \hat{x}_{1M} and \hat{x}_2 will be used in the Observer II with the assumption of negligibly small steady-state values of \tilde{x}_{1M} and \tilde{x}_2 .

Note: The film resistance (R_f) estimate convergence depends on nonzero current ($u \neq 0$). This is also evident from (9) as film the resistance is entering into the output equation as voltage drop $R_f u$.

Design of Observer II

In this part of the design we consider the whole Li-ion concentration dynamics of x_1 with unknown parameters θ and B_M . Here we consider estimate of \hat{x}_{1M} and \hat{x}_2 from the Observer I as available measurements. This partial dynamics can be written as:

$$\begin{aligned}\dot{\theta} &= 0 \\ \dot{B}_M &= 0 \\ \dot{x}_1 &= \theta f_1(x_2)Ax_1 + [0, \dots, 0, B_M]^T u \\ y_{1M} &= x_{1M} = Cx_1 \text{ where } C = [0, \dots, 0, 1]\end{aligned}\quad (13)$$

where x_1 is the whole Li-ion concentration vector as discussed before, θ and B_M are the unknown parameters augmented in the state vector, temperature x_2 is assumed to be known from the previous step, y_{1M} is \hat{x}_{1M} where we assume the steady-state error is negligible due to proper selection of gains in the Observer I.

The observer form is chosen as:

$$\begin{aligned}\dot{\hat{x}}_1 &= \theta f_1(x_2)A\hat{x}_1 + [0, \dots, 0, \hat{B}_M]^T u + L_4(y_{1M} - \hat{y}_{1M}) \\ \hat{y}_{1M} &= C\hat{x}_1\end{aligned}\quad (14)$$

The corresponding error dynamics is given as:

$$\begin{aligned}\dot{\tilde{x}}_1 &= \theta f_1(x_2)A\tilde{x}_1 - \theta f_1(x_2)A\hat{x}_1 + [0, \dots, 0, \hat{B}_M]^T u \\ &\quad - L_4\tilde{y}_{1M} \\ \tilde{y}_{1M} &= C\tilde{x}_1\end{aligned}\quad (15)$$

To analyze the stability of the error dynamics, the following Lyapunov function candidate has been chosen.

$$V = \frac{1}{2}\tilde{x}_1^T\tilde{x}_1 + \frac{1}{2}K_1\tilde{\theta}^2 + \frac{1}{2}K_2\tilde{B}_M^2 \quad (K_1, K_2 > 0)$$

Taking the derivative of the Lyapunov function candidate, (we drop the argument of the function f_1 for convenience)

$$\begin{aligned}\dot{V} &= \tilde{x}_1^T\dot{\tilde{x}}_1 + K_1\tilde{\theta}\dot{\tilde{\theta}} + K_2\tilde{B}_M\dot{\tilde{B}}_M \\ \Rightarrow \dot{V} &= \tilde{x}_1^T(\theta f_1 A\tilde{x}_1 - \theta f_1 A\hat{x}_1 - L_4\tilde{y}_{1M}) + \tilde{x}_1^T[0, \dots, \tilde{B}_M]^T u \\ &\quad + K_1\tilde{\theta}\dot{\tilde{\theta}} + K_2\tilde{B}_M\dot{\tilde{B}}_M \\ \Rightarrow \dot{V} &= \tilde{x}_1^T(\theta f_1 A\tilde{x}_1 + \tilde{\theta} f_1 A\hat{x}_1 - L_4 C\tilde{x}_1) + \tilde{y}_{1M}\tilde{B}_M u + K_1\tilde{\theta}\dot{\tilde{\theta}} \\ &\quad + K_2\tilde{B}_M\dot{\tilde{B}}_M \\ \Rightarrow \dot{V} &= \theta f_1 \tilde{x}_1^T A\tilde{x}_1 - \tilde{x}_1^T L_4 C\tilde{x}_1 + \tilde{x}_1^T \tilde{\theta} f_1 A\hat{x}_1 + K_1\tilde{\theta}\dot{\tilde{\theta}} + \tilde{y}_{1M}\tilde{B}_M u \\ &\quad + K_2\tilde{B}_M\dot{\tilde{B}}_M\end{aligned}$$

Using the assumption of slowly varying parameters ($\dot{\theta}, \dot{B}_M = 0$),

$$\begin{aligned}\dot{V} &= (\theta f_1 \tilde{x}_1^T A\tilde{x}_1 - \tilde{x}_1^T L_4 C\tilde{x}_1) \\ &\quad + \tilde{\theta} (f_1 \tilde{x}_1^T A\hat{x}_1 - K_1\tilde{\theta}) + \tilde{B}_M (\tilde{y}_{1M} u - K_2\dot{\tilde{B}}_M)\end{aligned}\quad (16)$$

Now, we choose the following adaptive laws, $\dot{\tilde{B}}_M = u\tilde{y}_{1M}/K_2$ and $\dot{\tilde{\theta}} = L_5\tilde{y}_{1M}/K_1$ where L_5 is yet to be determined. The third term on right hand side of (16) vanishes. Consider the second term on right hand side of (16):

$$\begin{aligned}\tilde{\theta}(f_1 \tilde{x}_1^T A\hat{x}_1 - L_5\tilde{y}_{1M}) \\ = \tilde{\theta}(f_1 \tilde{x}_1^T A\hat{x}_1 - L_5 C\tilde{x}_1) \\ = (f_1 \tilde{x}_1^T A\hat{x}_1 - L_5 C)\tilde{x}_1\tilde{\theta}\end{aligned}$$

To make the above term zero, the following conditions should be satisfied:

$$\begin{aligned}f_1 \tilde{x}_1^T A\hat{x}_1 = L_5 C \Rightarrow f_1 \tilde{x}_1^T A\hat{x}_1 C^T = L_5 C C^T \\ \Rightarrow L_5 = f_1 \tilde{x}_1^T A\hat{x}_1 C^T, \text{ as } C C^T = I.\end{aligned}$$

Therefore, the adaptation law becomes $\dot{\tilde{\theta}} = \frac{f_1 \tilde{x}_1^T A\hat{x}_1 C^T \tilde{y}_{1M}}{K_1}$.

The choice of these adaptation laws leads to the following Lyapunov function derivative,

$$\dot{V} = (\theta f_1 \tilde{x}_1^T A\tilde{x}_1 - \tilde{x}_1^T L_4 C\tilde{x}_1) \quad (17)$$

We choose L_4 such that $L_4 C$ becomes positive semidefinite leading to $-\tilde{x}_1^T L_4 C\tilde{x}_1 \leq 0$. Note that, $L_4 C$ cannot be negative definite given the structure of C . Now, from the Observation I it is known that A is negative semi-definite. Therefore, $\theta f_1 \tilde{x}_1^T A\tilde{x}_1 \leq 0$ as the function f_1 and unknown parameter θ are always positive from their physical properties. Therefore, from this analysis we can conclude that $\dot{V} = -\tilde{x}_1^T \beta \tilde{x}_1 \leq 0$. This proves the boundedness of the estimation errors \tilde{x}_1 , $\tilde{\theta}$ and \tilde{B}_M . Next, we attempt to analyze the asymptotic convergence of the errors to zero. To do so, we use a ‘‘Lyapunov-like’’ analysis based on Barbalat’s lemma [26], [27].

Asymptotic convergence of \tilde{x}_1 :

In this part, we will prove that $\dot{V} \rightarrow 0$ as $t \rightarrow \infty$ using Barbalat’s lemma. Lyapunov function candidate V is lower-bounded by choice and it is shown in the previous analysis that $\dot{V} \leq 0$. Uniform continuity of \dot{V} is equivalent to boundedness of \dot{V} which can be written as:

$$\begin{aligned}\dot{V} &= -2\tilde{x}_1^T \beta \tilde{x}_1, \text{ where} \\ \tilde{x}_1 &= \theta f_1(x_2)A\tilde{x}_1 - \theta f_1(x_2)A\hat{x}_1 + [0, \dots, 0, \tilde{B}_M]^T u - L_4 C\tilde{x}_1\end{aligned}$$

Now, x_1 , θ and f_1 are bounded from the physical properties of the system. Input u is also assumed to be bounded. From Lyapunov analysis it is shown that \tilde{x}_1 , $\tilde{\theta}$ and \tilde{B}_M are bounded. Therefore, \tilde{x}_1 and $\tilde{\theta}$ are also bounded. So, it can be concluded that \dot{V} is bounded which in turn proves that \dot{V} is bounded. Therefore, from Barbalat’s lemma it can be concluded that $\dot{V} \rightarrow 0$ as $t \rightarrow \infty$. Then, using \dot{V} expression (17), it can be shown that $\tilde{x}_1 \rightarrow 0$ asymptotically.

Asymptotic convergence of $\tilde{\theta}$ and \tilde{B}_M :

In this part, we will prove that $\dot{\tilde{x}}_1 \rightarrow 0$ as $t \rightarrow \infty$ using Barbalat’s lemma. It is already shown that $\tilde{x}_1 \rightarrow 0$ as $t \rightarrow \infty$. The limit,

$$\int_0^\infty \dot{\tilde{x}}_1 dt = \lim_{t \rightarrow \infty} \tilde{x}_1(t) - \tilde{x}_1(0) = -\tilde{x}_1(0)$$

exists and is finite. With the signals already shown bounded in the previous step and additionally assuming \dot{u} bounded, it can be shown that $\dot{\tilde{x}}_1$ is bounded. This leads to the fact that $\dot{\tilde{x}}_1 \rightarrow 0$ as $t \rightarrow \infty$. Considering the $\dot{\tilde{x}}_1$ expression with $\tilde{x}_1 \rightarrow 0$,

$$\dot{\tilde{x}}_1 = \tilde{\theta} f_1(x_2)A\tilde{x}_1 + [0, \dots, 0, \tilde{B}_M]^T u$$

As $\tilde{x}_1 \rightarrow 0$, the expression boils down to:

$$\begin{aligned}\tilde{\theta} f_1(x_2)A\tilde{x}_1 + [0, \dots, 0, \tilde{B}_M]^T u &= 0 \\ \Rightarrow f_1(x_2)A\tilde{x}_1\tilde{\theta} + [0, \dots, 0, u]^T \tilde{B}_M &= 0 \\ \Rightarrow [[f_1(x_2)A\tilde{x}_1] \quad [0, \dots, 0, u]^T]_{M \times 2} \begin{bmatrix} \tilde{\theta} \\ \tilde{B}_M \end{bmatrix}_{2 \times 1} &= 0\end{aligned}$$

$$\Rightarrow X_M \times 2 \begin{bmatrix} \tilde{\theta} \\ \tilde{B}_M \end{bmatrix}_{2 \times 1} = 0, \text{ with } X = [[f_1(x_2)Ax_1] \quad [0, \dots, u]^T]$$

$$\Rightarrow [X^T X]_{2 \times 2} \begin{bmatrix} \tilde{\theta} \\ \tilde{B}_M \end{bmatrix}_{2 \times 1} = 0$$

It can be concluded that $\tilde{\theta}, \tilde{B}_M \rightarrow 0$ as $t \rightarrow \infty$ under the condition $|X^T X| \neq 0$, which leads to the condition $u \neq 0$. Note that, the convergence of the parameter estimates to their true values depends on certain persistently exciting input current.

Note: The analysis on asymptotic convergence of $\tilde{x}_1, \tilde{\theta}$ and \tilde{B}_M is carried out based on the assumption that Observer I provides accurate estimate of the surface concentration. However, there will always be a steady-state error in reality. Although this steady-state error can be neglected for all practical purposes, $\tilde{x}_1, \tilde{\theta}$ and \tilde{B}_M will converge to a small nonzero value in reality.

Systematic Approach for Observer Gains Selection

Selection of observer gains in this design is of great importance for the convergence of state and parameter estimates. A systematic approach for gain selection is provided for implementation of this overall adaptive scheme.

Observer I:

Step I: Select an arbitrary positive value for gain L_1 and then correspondingly select L_3 satisfying the condition $L_1 |\tilde{x}_{1M}|_{max} |u|_{max} < L_3$ where $|u|_{max}$ is the guess of maximum possible current and $|\tilde{x}_{1M}|_{max}$ is guess of maximum possible value of state error. Check the convergence rate and steady-state value of the estimation errors \tilde{x}_{1M} and \tilde{R}_f . Increase gain L_1 and correspondingly L_3 until acceptable convergence rates and steady-state errors are achieved.

Step II: Selection of L_2 is independent of other gains. Initialize L_2 by an arbitrary high value and increase it until acceptable convergence rate of \tilde{x}_2 and steady-state error are achieved.

Observer II:

Step III: Select an arbitrary $L_4 = \sigma [1, \dots, 1]^T$ with a scalar parameter $\sigma > 0$ such that $L_4 C$ is positive semidefinite. Then keep increasing σ until acceptable convergence rate is achieved.

Step IV: For a given selection of L_4 , parameter adaptation law gains K_1 and K_2 should be tuned together. This is because these two gains are observed to have a strong inter-dependence. Initialize K_1 and K_2 with an arbitrary small positive numbers and then keep increasing both of them in steps until acceptable convergence rates are achieved. The user should take care that the selection of K_1 and K_2 should not significantly impact the \tilde{x}_1 convergence given by L_4 .

RESULTS & DISCUSSIONS

In this section, the performance of the adaptive observer scheme is demonstrated via simulation studies. In this study, the SPM model with both positive and negative electrode dynamics is used as plant model. Model parameter values of Li-ion cell have been taken from [9] and [22]. To emulate realistic

scenario, 1 mV and 1°C variance noise is added to the voltage and temperature measurement, respectively. A noise component of 1 mA is also added to the current measurement. Besides emulating realistic measurement scenario this noise component also helps in maintaining persistently exciting input signal.

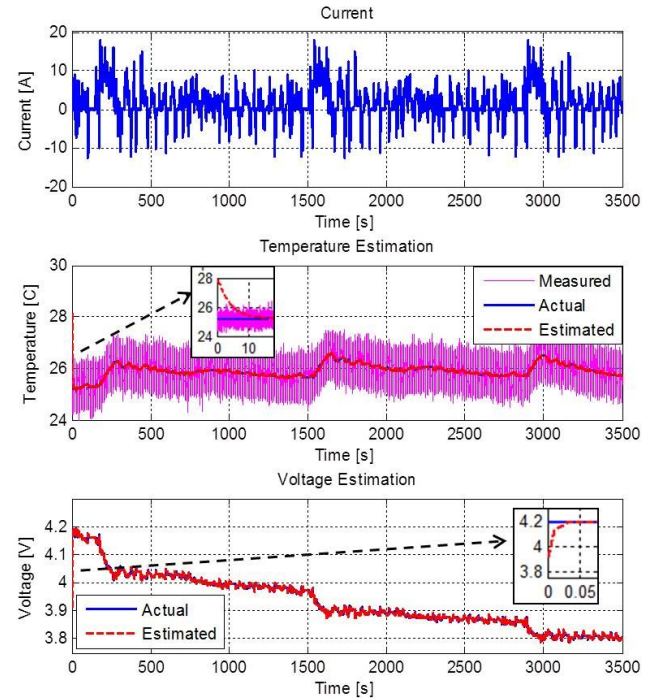


Figure 4: Temperature and Voltage Estimation Performance

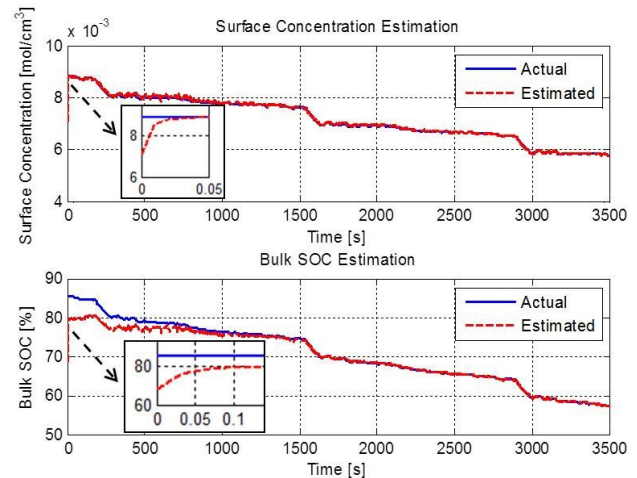


Figure 5: Bulk SOC and Surface Concentration Estimation Performance

To evaluate the error convergence, state and parameter estimates are initialized with different initial conditions than that of actual plant. The performance of the state and parameter estimation is shown in Figures 4, 5 and 6 for a repeated UDDS (Urban Dynamometer Driving Cycle) cycle. UDDS is

originally a velocity profile for testing a full-size vehicle, from which a scaled-down current profile is constructed.

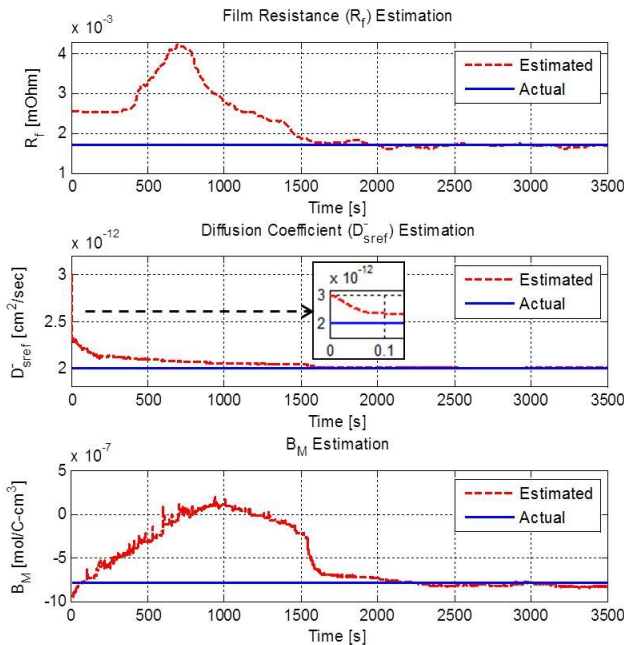


Figure 6: Parameter Estimation Performance

In Fig. 4, it is clearly shown that the temperature observer is able to estimate the actual temperature with negligible steady-state error despite noisy measurement and uncertainties. In Fig. 5, it can be seen that Observer I is able to estimate surface concentration (also the voltage given in Fig. 4) with a fast convergence rate and negligible steady-state error. Note that, this fast convergence is desired as the surface concentration estimate is being used by Observer II to estimate the rest of the states and parameters.

The bulk SOC estimation performance is also shown in Fig. 5. Note that, initially the convergence rate is much faster although it slows down later. This is because the surface concentration observer (Observer I) has a much faster convergence rate than the Observer II that estimates the rest of the node concentrations. Therefore, all other estimated node concentrations except for the surface one, converge in a slower manner leading to slower convergence of the bulk SOC. This difference of the convergence rates of the two observers is due to our particular selection of gains. Parameter estimation performance is shown in Fig. 6 from which it can be concluded that the estimates converge with a reasonable accuracy. The convergence rates for the parameter estimates are much slower than those of the states. However, this should not be a problem due to the time scale separation between states and parameters. One observation we made is that the overall performance of the adaptive scheme degrades with high initial error \hat{B}_M . Higher initial error in that particular parameter may lead to the divergence of the estimates. This is one of the limitations of this scheme.

CONCLUSION

In this paper, an adaptive observer design is presented for simultaneous state-parameter estimation of a Li-ion cell. This design considers the coupling between electrochemical and thermal dynamics of the cell. The observer design is split into two parts to simplify the design. The parts are designed separately based on Lyapunov's stability analysis and a systematic approach is provided for the selection of the gains. Simulation studies show the effectiveness of the design where the states and parameters are estimated with a desired convergence rate and accuracy.

However, it should be mentioned that there are some limitations for this adaptive observer scheme. Firstly, the stability of the overall scheme is not guaranteed under zero input current which essentially translates to requiring persistent excitation of the input. Next, high initial error in B_M estimate degrades the performance of the scheme.

As future work, extension of this design can be evaluated with estimation of other physical parameters of the cell including other uncertainties. Moreover, experimental studies are planned on a physical Li-ion cell to validate this design.

ACKNOWLEDGMENTS

This research is supported, in part, by the US Department of Energy GATE program under grant number DE-EE0005571 and NSF under grant number CMMI-1055254.

REFERENCES

- [1] Hatzell, K. B., Sharma, A., and Fathy, H. K., 2012. "A survey of long-term health modeling, estimation, and control of Lithium-ion batteries: Challenges and opportunities". in 2012 American Control Conference (ACC), pp. 584-591.
- [2] Saha, B., Goebel, K., Poll, S., and Christophersen, J., 2007. "An integrated approach to battery health monitoring using bayesian regression and state estimation". In 2007 IEEE Autotestcon, pp. 646-653.
- [3] Ng, K. S., Moo, C., Chen, Y., and Hsieh, Y., 2009. "Enhanced coulomb counting method for estimating state-of-charge and state-of-health of lithium-ion batteries". *Applied Energy*, vol. 86, no. 9, pp. 1506-1511.
- [4] Plett, G. L., 2004. "Extended Kalman filtering for battery management systems of LiPB-based HEV battery packs: Part 3. State and parameter estimation". *Journal of Power sources*, vol. 134, no. 2, pp. 277-292.
- [5] Remmlinger, J., Buchholz, M., Meiler, M., Bernreuter, P., and Dietmayer, K., 2011. "State-of-health monitoring of lithium-ion batteries in electric vehicles by on-board internal resistance estimation". *Journal of Power Sources*, vol. 196, no. 12, pp. 5357-5363.
- [6] Kim, Il-Song, 2010. "A Technique for Estimating the State of Health of Lithium Batteries Through a Dual-Sliding-Mode Observer". *IEEE Transactions on Power Electronics*, vol.25, no.4, pp.1013-1022.
- [7] Chaturvedi, N. A., Klein, R., Christensen, J., Ahmed, J., and Kojic, A., 2010. "Algorithms for Advanced Battery-

- Management Systems”. *IEEE Control Systems Magazine*, vol.30, no.3, pp.49-68.
- [8] Doyle, M., Fuller, T. F., and Newman, J., 1993. “Modeling of galvanostatic charge and discharge of the lithium/polymer/insertion cell”. *Journal of the Electrochemical Society*, vol. 140, no. 6, pp. 1526-1533.
- [9] Smith, K. A., Rahn, C. D., and Wang, C., 2010. “Model-based electrochemical estimation and constraint management for pulse operation of lithium ion batteries”. *IEEE Transactions on Control Systems Technology*, vol. 18, no. 3, pp. 654-663.
- [10] Klein, R.; Chaturvedi, N.A.; Christensen, J.; Ahmed, J.; Findeisen, R.; Kojic, A., 2013. “Electrochemical Model Based Observer Design for a Lithium-Ion Battery”. *IEEE Transactions on Control Systems Technology*, vol.21, no. 2, pp. 289-301.
- [11] Santhanagopalan, S., and White, R. E., 2006. “Online estimation of the state of charge of a lithium ion cell”. *Journal of Power Sources*, vol. 161, no. 2, pp. 1346-1355.
- [12] Domenico, D., Stefanopoulou, A., and Fiengo, G., 2010. “Lithium-ion battery state of charge and critical surface charge estimation using an electrochemical model-based extended Kalman filter”. *ASME Journal of Dynamic Systems, Measurement, and Control*, vol. 132, no. 6, pp. 061302.
- [13] Moura, S. J., Chaturvedi, N. A., and Krstic, M., 2012. “PDE estimation techniques for advanced battery management systems—Part I: SOC estimation”. In 2012 American Control Conference (ACC), pp. 559-565.
- [14] Dey, S., and Ayalew, B., “Nonlinear Observer Designs for State-of-Charge Estimation of Lithium-ion Batteries”. In 2014 American Control Conference(ACC),pp.248-253.
- [15] Samadi, M. F., Alavi, S. M., and Saif, M., 2013. “Online state and parameter estimation of the Li-ion battery in a Bayesian framework”. In 2013 American Control Conference (ACC), pp. 4693-4698.
- [16] Schmidt, A. P., Bitzer, M., Imre, Á. W., and Guzzella, L., 2010. “Model-based distinction and quantification of capacity loss and rate capability fade in Li-ion batteries”. *Journal of Power Sources*, vol. 195, no. 22, pp. 7634-7638.
- [17] Fang, H., Wang, Y., Sahinoglu, Z., Wada, T., and Hara, S., 2013. “Adaptive estimation of state of charge for lithium-ion batteries”. In 2013 American Control Conference (ACC), pp. 3485-3491.
- [18] Fang, H., Wang, Y., Sahinoglu, Z., Wada, T., and Hara, S., 2014. “State of charge estimation for lithium-ion batteries: An adaptive approach”. *Control Engineering Practice*, vol. 25, pp. 45-54.
- [19] Moura, S. J., Chaturvedi, N. A., and Krstic, M., 2013. “Adaptive PDE Observer for Battery SOC/SOH Estimation via an Electrochemical Model”. *ASME Journal of Dynamic Systems, Measurement, and Control*, vol. 136, no. 1.
- [20] Dey, S., Ayalew, B., and Pisu, P., 2014. “Combined Estimation of State-of-Charge and State-of-Health of Li-ion Battery Cells Using SMO on Electrochemical Model.” accepted in 13th International Workshop on Variable Structure Systems.
- [21] Klein, R., Chaturvedi, N.A., Christensen, J., Ahmed, J., Findeisen, R., and Kojic, A., 2010. “State estimation of a reduced electrochemical model of a lithium-ion battery”. In 2010 American Control Conference (ACC), pp. 6618-6623.
- [22] Guo, M., Sikha, G., and White, R.E., 2011. “Single-particle model for a lithium-ion cell: thermal behavior”. *Journal of The Electrochemical Society*, vol. 158, no. 2, pp. A122-A132.
- [23] Ramadass, P., Haran, B., White, R., Popov, B. N., 2003. “Mathematical modeling of the capacity fade of Li-ion cells”. *Journal of Power Sources*, vol. 123, no. 2, pp. 230-240.
- [24] Vetter, J., Novák, P., Wagner, M.R., Veit, C., Möller, K.-C., Besenhard, J.O., Winter, M., Wohlfahrt-Mehrens, M., Vogler, C., Hammouche, A., 2005. “Ageing mechanisms in lithium-ion batteries”. *Journal of Power Sources*, vol. 147, no. 1–2, Pages 269-281.
- [25] Bandhauer, T. M., Garimella, S., and Fuller, T. F., 2011. “A critical review of thermal issues in lithium-ion batteries”. *Journal of the Electrochemical Society*, vol. 158, no. 3, pp. R1-R25.
- [26] Slotine, J. J. E., & Li, W., 1991. *Applied nonlinear control*. Upper Saddle River, NJ: Prentice Hall.
- [27] Narendra, K. S. and Annaswamy, A., 1989. *Stable Adaptive Systems*. Englewood Cliffs, NJ: Prentice-Hall.